Available online at www.sciencedirect.com

ScienceDirect

Procedia Materials Science 6 (2014) 821 – 834

Procedia Materials Science

www.elsevier.com/locate/procedia

3rd International Conference on Materials Processing and Characterisation (ICMPC 2014)

Analytical Modeling of Temperature Distribution, Peak Temperature, Cooling Rate and Thermal Cycles in a Solid Work Piece Welded By Laser Welding Process

K.Suresh Kumar[a,b]*

[a] *Research Scholar,University of Madras, Chennai,Tamil Nadu,600005,India*
[b]*P.T.LeeChengalvaraya Naicker College of Engineering and Technology,Kanchipuram,Tamil Nadu,631502,India*

Abstract

Generalized theoretical prediction of temperature distribution, peak temperature, cooling rate and thermal cycles in a solid work piece welded by laser welding process, where no melting is occurs, i.e., from the boundary of fusion zone to the end of heat affected zone. With the moving point or line heat source may be considered for the analysis that indicates the temperature gradient ahead of the heat source is much higher than that behind, increasing welding velocity elongates the isotherms surrounding the heat source, higher thermal conductivity of materials make the isotherm more circular, reducing the temperature gradient in front of the heat source. The peak temperature experienced throughout the workpiece, determine the size of the heat affected zone (HAZ). The peak temperature at a given point is experienced by the point shortly after it is passed by the heat source. The size of the HAZ increases with the net energy input. The cooling rates experienced by a material, determines the grain structure and phases that are formed. Increasing the heat input reduces the cooling rate. While increasing the welding velocity increases the cooling rate. Higher thickness, thermal conductivity of the material also increases the cooling rate.

Selection and peer review under responsibility of the Gokaraju Rangaraju Institute of Engineering and Technology (GRIET)

Keywords: Laser Beam Welding, Heat Affected Zone, Temperature Distribution, Cooling Rate, Peak Temperature, Thermal Cycle.

* Corresponding author. Tel.:+ 919865810987
E-mail address: lectsuresh25@gmail.com

Selection and peer review under responsibility of the Gokaraju Rangaraju Institute of Engineering and Technology (GRIET)
doi:10.1016/j.mspro.2014.07.099

1. Introduction

Laser beam welding process has numerous advantages compared to the conventional welding processes. Due to high intensity of its localised heat source, a nonuniform transient temperature field occurs, Klaus Zimmer (2009). This field initially causes a rapid thermal expansion followed by a thermal contraction of the laser irradiated materials during welding.

Nomenclature

Q	The heat flux or rate of heat flow per unit area across the surface in W/mm^2
K	A constant, coefficient of thermal conductivity in W/mm/K
A	The unit area of cross section perpendicular to the flow of heat in mm^2
T	The increase in temperature above the surroundings in Kelvin
T_0	Ambient temperature in Kelvin
$\partial T/(\partial x)$	Temperature gradient with respect to distance from the point of irradiation in K/mm
ρ	(= $m/A\delta x$) The density of a medium in kg/m^3
m	Mass of a substance in kg
v	(= $A\delta x$) Volume of a substance in mm^3
C_p	Specific heat capacity of a substance in J/KgK
E	Emissivity power of the surface
P	Perimeter of a work piece in mm
Q_g	(=H/K) Rate of internal heat generation in a work piece in W/mm^2
∇	Laplacian operator
α	(=$K/\rho s$) Thermal diffusivity of a work piece in mm^2/sec
$\partial T/\partial t$	The time rate of change of temperature in the moving coordinate system in K/sec.
x, y, z	A coordinate system with origin "O".
ξ, y', z'	Transformed coordinate system with origin "O".
h	The plate thickness of the work piece in mm
U_x	Welding velocity in x-direction in mm/s.
r	The radius of a cylinder drawn around the heat source in mm
$K_0(\chi)$	The modified Bessel function of the second kind of order zero
e	Natural exponent (= 2.71828)
T_p	The peak or maximum temperature at a distance Y from the fusion boundary in Kelvin
Y	The distance from the fusion boundary at the workpiece surface in mm
T_m	Melting point of the work piece in Kelvin

The severity of the induced temperature gradients and the degree of restraint the joint imposes on the thermal deformation determine the residual state of the weldment when it has finally cooled, Moraitis G.A and G.N. Labeas, (2008). This residual state is characterized by a combination of internally balanced residual stresses and weld distortion. Residual stresses and weld distortion in a weld joint occur throughout the area of solidified weld metal and the heat affected zone. Both the magnitudes and the distributions of the residual stresses are taken into account to accurate estimate a weldment's fatigue life, Shah ram Sarkani et al. (2000). Mathematical models have been developed, computed and simulated and also validated through experimental results, are of major importance for a high number of reasons: the deep understanding of the laser welding physics, reliable extension of the process applicability to modern demanding industrial applications and to optimize the process parameters, with less cost penalty, Moraitis G.A and G.N. Labeas (2009).

2. Brief History about Modelling of Laser Welding

Researchers have studied the laser welding process since the early 1970s and several mathematical models have been developed. Rosenthal (1946) and many other authors, have studied classical solutions of the heat conduction equations. Carslaw and Jaeger (1959) have brought this together in a complete reference book with analytical solutions of the heat conduction equations. The heat sources used are point sources, line sources and plane sources, since these are the only types of geometry were analytical solutions are straightforward to obtain. This type of sources is suited to predict the thermal history at a large distance from the source. K.N.Lanakala palli et al. (1996) reviewed the range of mathematical models for laser welding associated with a number of different parameters used for deriving the governing equations until 1995. S.E.Chidiac and F.A.Mirza (1993) were developed 3D heat flow model for Arc welding to determine the thermal cyclic response for various materials and for different types of welding arcs. The most common problem of welding dissimilar metals with respect to residual stresses is the differences in the coefficient of thermal expansion and thermal conductivity of the two welded metals, Anawa E.M and A.G.Olabi (2008). S. Murugan et al. (1998) investigated the temperature distribution, thermal cycles of the bead on plates weld joint welded with MMA method by single pass and with multipass, since thermal cycles cause microstructural changes, subsequently, arise the residual stresses which affect the performance the welded components. In another publication, S. Murugan et al. (1999) also calculated the experimental temperature distribution for different thickness of plates of dissimilar multipass welding and those hints to establish the microstructural changes, phase transformation and degradation studies from results of average peak temperatures. M.R. Frewin and D.A. Scott, (1999) were developed a model to estimate the temperature contours as function of time during pulsed laser welding in addition to the measurement of fusion zone and heat affected zone. Most of the heat transfer models developed until the year 2002 was reviewed by A.P. Mackwood and R.C. Crafer (2005). S. Sarkani et al. (2000) reported the possibility of replacing a computationally expensive 3D FE analysis of welding temperature distribution in the central zone and residual stresses with a less expensive 2D and validated with single pass multipass T-Joint welding. Wenchun et al. (2009) modelled the temperature history and residual stress of vacuum brazed stainless steel plate-fin structure by Finite Element Analysis with ABAQUS code. B.S.Yilbas et al.

(2010) consecutive publications on modeling of temperature and thermal stress field distribution using FEA with ANSYS code for low carbon steel and alumina. M. Van Elsen et al. (2007) effectively used the analytical and numerical solutions of the heat conduction equations to calculate the temperature distribution in a semi-infinite medium for a localised moving 3D heat source of any type for use in laser material processing, as welding, layered manufacturing and laser alloying. Martinson et al. (2009) stated that phase transformation due to different cooling rates is important when dealing with high strength or advanced high–strength steels which are seeing increasing use in the car industry. Jaroslav Mackerle, (2004) have been published many bibliography that provides hundreds of references until from the year 1976 to 2004 on modelling and analysis of Laser beam welding of 2D, 3D thermo mechanical, to evaluate temperature, stress and distortion distributions, linear and non-linear analysis, phase change problems, solidification, melting, austenitic-martensitic phase change, martensitic transformation, solid liquid phase transformation etc., including welding under consideration of austenitic stainless steel and other metals and alloys.

In this paper, the main objective is to present the generalized analytical model to predict the temperature distribution, peak temperature, cooling rates and thermal cycles from the boundary of fusion zone to the end of heat affected zone of a weld-joint welded by laser welding.

2. Heat Flux Conduction Equation in a Laser Irradiated Work Piece

During laser beam welding process, heat can be transferred from one part of the materials to another part by three different ways viz conduction, convection and radiation. If heat is transmitted by the actual movement of the heated particles, the processes is known as conviction, which is prominent in the case of liquids and gases. Radiation, the heat transferred from materials surface to the surroundings directly without the necessity of the intervening medium.

When laser beam irradiated on a metal slab which start to conduct heat energy, the molecules at the surface vibrate with higher amplitude (kinetic energy) and transmit the heat energy from one particle to another and so on without actual motion of the particles, known as conduction.

According to the Fourier first law of heat conduction in a rectangular metal slab is

$$Q = -KA\frac{dT}{dx} \quad \text{-------- (1)}$$

Hence, heat transmitted per second by the metal slab between any two points at the distance δx is given by

$$Q = KA\frac{\partial^2 T}{\partial x^2}\delta x \quad \text{------ (2)}$$

Before the steady state is reached, the quantity of heat Q is used in two ways before steady state is reached. Partly the heat is used to raise the temperature of the metal slab and the rest is lost due to radiation. The heat used per second to raise the temperature of the metal slab is

= Mass X Specific heat X Rate of raise of temperature

$$= (A\delta x)\rho Cp\frac{\partial T}{\partial t} \quad \text{------ (3)}$$

The heat lost per second due to radiation in from the surface of the metal slab

$= EP\delta xT$ ------- (4)

Where E is emissivity power of the surface, P is perimeter and T is average excess of temperature of the metal slab between any two points considered.

To obtain the temperature distribution as function of time, we consider control volume as shown in the figure 1.

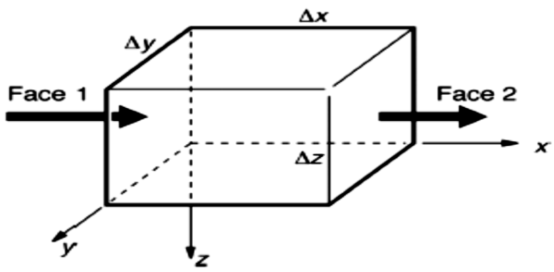

Figure 1: Heat flow in a control volume

Considering the law of conservation of energy, the rate of change of internal energy ($Q_g = \frac{H}{K}$, which is also known as the internal heat generation, ratio of amount heat 'H' to thermal conductivity 'K') per unit volume of the control volume must be equal to the sum of the net rate of heat flux per unit volume across its faces and any heat sources or sink with in it per volume such as chemical reactions or current passing through it (Joule effect).

Hence, the heat balance on the differential element can be stated that rate of heat conduction and the internal heat generation are equal to the heat convection and radiation.

$$\left(KA\frac{\partial^2 T}{\partial x^2}\delta x\right) + Q_g = (A\delta x)\rho S\frac{\partial T}{\partial t} + EP\delta xT \qquad \text{(or)}$$

$$\left(\frac{\partial^2 T}{\partial x^2}\right) + Q_g = \frac{\rho s}{K}\frac{\partial T}{\partial t} + \frac{EP}{KA}T \qquad \text{----- (5)}$$

The rectilinear flow of heat along a rectangular metal slab in three dimensions in terms of Cartesian coordinates is

$$\left(\frac{\partial^2 T}{\partial x^2} + \frac{\partial^2 T}{\partial y^2} + \frac{\partial^2 T}{\partial z^2}\right) + Q_g = \frac{\rho s}{K}\frac{\partial T}{\partial t} + \frac{EP}{KA}T \qquad \text{----- (6)}$$

In a more compact form,

$$\nabla^2 T + Q_g = \frac{1}{\alpha}\frac{\partial T}{\partial t} + \frac{EP}{KA}T \qquad \text{----- (7)}$$

Where, $\nabla^2 = \frac{\partial^2}{\partial x^2} + \frac{\partial^2}{\partial y^2} + \frac{\partial^2}{\partial z^2}$ is laplacian operator.

Thermal diffusivity or Thermometric conductivity (α): It's defined as ratio of thermal conductivity to thermal capacity per unit volume

$$\alpha = \frac{K}{\rho s} \qquad \text{----- (8)}$$

Under steady state flow of heat $\frac{\partial T}{\partial t} = 0$, therefore, hence, the equation (7) can reduced as follows,

$$\frac{\partial^2 T}{\partial x^2} + \frac{\partial^2 T}{\partial y^2} + \frac{\partial^2 T}{\partial z^2} = 0 \qquad \text{------ (9)}$$

Equation (9) is known as Laplacian transformation.

In the case of transient heat conduction, If the surface of the material is assumed that it is impervious to heat flow has arbitrary of temperature in the direction of x and y, independent of z (Since, there is no heat flow in z direction actually which is perpendicular direction to laser beam incident on materials surface). From the assumptions,

$$\frac{\partial^2 T}{\partial z^2} = 0 \text{ and } \frac{EP}{KA}T = 0$$

Hence, the equation (7) can reduced as follows,

$$\frac{\partial^2 T}{\partial x^2} + \frac{\partial^2 T}{\partial y^2} + Q_g = \frac{1}{\alpha}\frac{\partial T}{\partial t} \qquad \text{------ (10)}$$

Now, the above expression is reduced to the two dimensional equation for rectilinear flow of heat along a rectangular metal slab in terms of Cartesian coordinates. In this simplified lumped parameter energy balance equations are presented that enable quick estimates to be made of energy requirements for a given laser welding process. This differential equation with its associated boundary conditions can be solved using analytical or numerical methods such as the finite difference, finite element or control volume methods, S. Murugan et al. (1998).

3. Temperature Distribution in a Laser Welding Process

Generally, the solution of heat flow equations for any welding conditions is a complicated problem. In order to find analytical solutions to the equations, it is therefore necessary to make many simplifying assumptions. To make the problem more tractable analytically, the following assumptions are made,

1. The workpiece material is assumed to be homogeneous and isotropic.
2. Heat conduction through the workpiece is usually much greater than any heat exchange with the surroundings by natural convection or radiation. It is further assumed that the workpiece surfaces are adiabatic; that is, there is no heat loss or gain by either convection or radiation.
3. The heat source is considered to be a moving line that goes through the entire plate thickness uniformly.
4. A Gaussian distribution that is more representative of the heat source is then considered. TEM_{00} spatial mode most suitable specifically for welding, also for cutting and drilling.
5. Analysis of the moving heat source case is facilitated by using a coordinate system that is attached to the heat source.
6. In a realistic model the thermal conductivity and specific heat should be considered as functions of temperature. The equation is linearized by assuming that the material's physical coefficients such as thermal conductivity are independent of temperature. Even though the thermal conductivity for plain carbon steel, for example, may vary from about 65 W/m K at 0˚C to about 30 W/m K at 1200˚C, using an average value (about 50 W/m K) provides a reasonable approximation and enables a closed form solution to be obtained. Thus $\partial k/\partial T = 0$.
7. The internal heat generation is neglected. This means $Q_g = 0$. This assumption is reasonable for a number of applications, especially when one compares the external heat sources associated with some

laser processes with any heat that might be generated within the material. However, this is not necessarily true of oxygen assisted laser cutting where the exothermic reaction can be considerable.

8. In most types of welding, melting occurs and convective heat transfer in addition to conductive heat transfer takes place. In addition, most realistic welding problems have heat losses at the boundaries caused by convection, radiation and contact with other bodies, so the precise boundary conditions are often unknown.
9. No phase changes occur; that is, the effect of latent heat of fusion is negligible. The major drawback lies in the fact that the behaviour of molten material cannot be taken into account.

Let us, therefore, consider a coordinate system moving with the heat source along the x-axis, as shown in Figure 2. The corresponding governing equation is obtained by a coordinate transformation from the plate to the heat source, with x being replaced by ξ, y by y′, z by z′, and t by t′, that is,

$$\xi = x - u_x t,\ y' = y,\ z' = z,\ t' = t$$

Where, u_x is the traverse velocity of the heat source in the x-direction (mm/s).

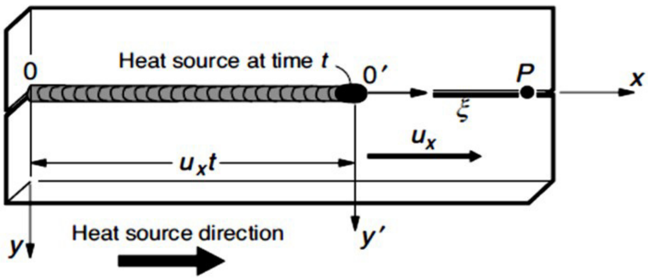

Figure 2: Schematic of moving coordinate system associated with laser processing

where ξ, y, z is a coordinate system attached to the moving heat source, with positive ξ in the direction in which the heat source is moving; x, y, z is a coordinate system with origin O and fixed to the workpiece, with positive x in the direction in which the heat source is moving; and ∂T/∂t is the time rate of change of temperature in the moving coordinate system. Since the heat source is uniform through the thickness, there can be no change in temperature in the thickness direction.

The Gaussian heat source is considered separately for two forms of solutions:

1. One case is that of a thick plate on which a point heat source moves and involves three-dimensional heat flow. This might be the case, for example, in conduction mode welding.

2. The other case is that of a thin plate with a line heat source that penetrates through the thickness and involves two-dimensional heat flow. Examples would be keyhole welding or laser cutting.

To determine whether a plate is thin or thick, the following equation may be used as an initial approximation:

$$\beta_c = h\sqrt{\frac{\rho C_p\, U_x (T - T_0)}{Q}} \text{ ------ (11)}$$

The plate is considered to be thin when βc < 0.6 and thick when βc > 0.9. When high accuracy is desired and 0.6 < βc < 0.9, then it is best to solve the equations numerically.

4. Temperature Distribution of a Weld Plate with Moving Heat Source

The configuration for this case is illustrated schematically in Figure 3. In this case, heat flow is in two directions ξ (or x)-direction and y-direction. There is no flow in the z-direction.

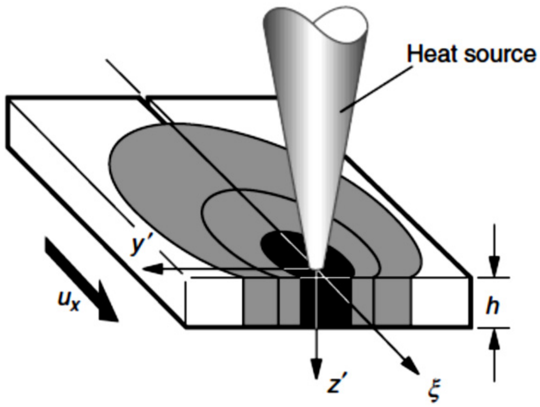

Figure 3: Two-dimensional conduction mode laser beam, (Andrzej Sluzalec, (2005)).

The heat source is considered to be a line that goes through the entire plate thickness uniformly. Thus, heat is input to the system as power per unit thickness. Now let r $=\sqrt{\xi^2 + y^2}$, the radius of a cylinder drawn around the heat source. Since the heat source is uniform through the thickness, there can be no change in temperature in the thickness direction. Thus, we have

$\frac{\partial T}{\partial x}= 0$ for all z

The temperature distribution in a plate for a moving line heat source (John Michael Dowden, 2001) is given as

$$T - T_0 = \frac{Q}{2\pi k\alpha} \exp\left(-\frac{U_x \xi}{2k}\right) K_0 \left(\frac{U_x r}{2k}\right) \text{------ (12)}$$

Where K_0 (χ) is the modified Bessel function of the second kind of order zero.

Equation (12) is also sometimes known as the Rosenthal equation, before Carslaw and Jaeger (1959) who first derived them. Samples of the temperature distribution as represented by a family of isotherms drawn around the instantaneous heat source position (x − y plane) are shown in Figures 4 shows the effect of thermal conductivity by comparing the isotherms for a relatively low thermal conductivity material (say steel) and a relatively high thermal conductivity material (say aluminum) when other processing conditions are the same. Figure 4 shows the effect of speed on the isotherms, for the same input power. Finally, Figure 4 compares the isotherms obtained for a thin plate and a thick plate, when the processing conditions are the same.

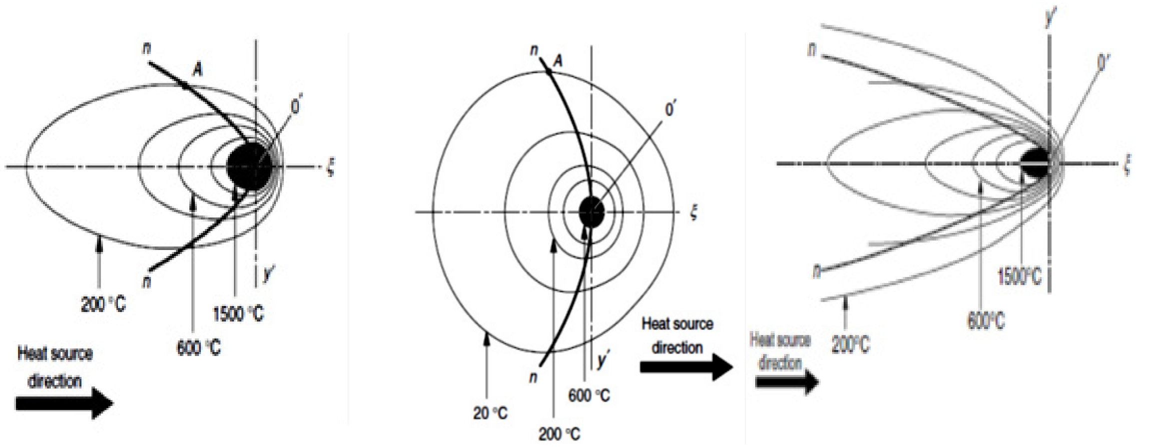

(4.1a) (4.2a) (4.3a)

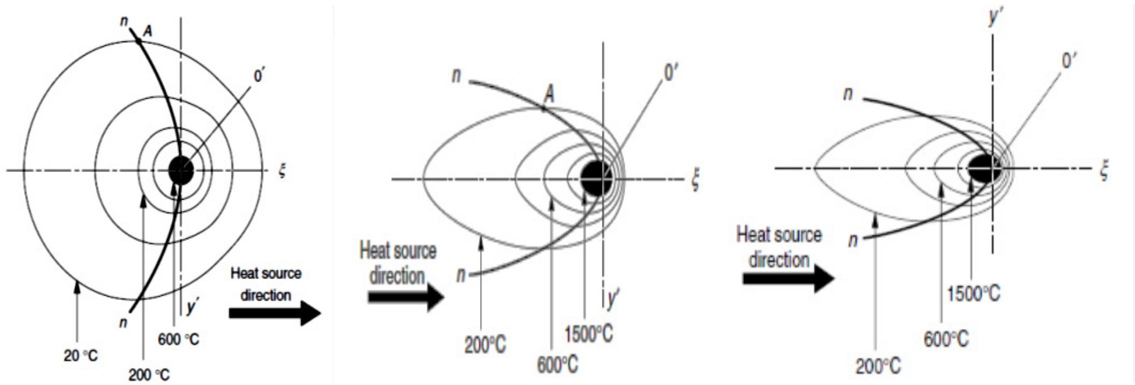

(4.1b) (4.2b) (4.3b)

Figure 4**:** Temperature distributions in a plate for (4.1a) low thermal conductivity low carbon steel and (4.1b) high thermal conductivity aluminum, Temperature distributions as a function of processing speed (4.2a) Low speed. (4.2b) High speed (doubled) and Temperature distribution as a function of plate thickness, other processing conditions being the same. (4.3a) Thin plate. (4.3b) Thick plate (more than 20 times thicker), (D. Rosenthal, (1946).

These graphs were obtained by solving equations (12). From these figures and the equations, the following deductions can be made:

1. The temperature gradient ahead of the heat source is much higher than that behind it.

2. Different points along the y-axis in a given section reach their peak temperature at different times. Points farther away have a lower peak temperature, and that is reached at a later time. The locus of points that reach their peak temperatures at the same instant is indicated by curve n - n in Figure 4 The curve bends backward. This is due to the finite time that it takes for heat to flow in materials, which delays the occurrence of the peak temperature at

points along the y-axis. Curve n - n also separates points in the plate with rising temperature from those with falling temperature. Its shape depends on both the traverse speed and the thermal diffusivity of the material.

3. A higher thermal conductivity material such as aluminum makes the isotherms more circular, reducing the temperature gradient in front of the heat source, 4.1a and 4.1b of figure 4.

4. Increasing the traverse speed makes the isotherms more elongated, while also increasing the lag of the locus n - n, 4.2a and 4.2b figure 4.

5. Increasing the heat input or preheating does not change the shape of the isotherm but increases the size. This widens the fusion zone, as well as the heat-affected zone (HAZ).

6. For the same conditions, a thinner plate results in a greater heat affected zone size than a thicker plate, while the thicker plate results in a higher temperature gradient, 4.3a and 4.3b of figure 4**.**

5. Peak Temperature

The peak temperature at a given point is experienced by the point shortly after it is passed by the heat source, S. Murugan et al. (1998). This is evident from an isotherm (locus of points with the same temperature) of the temperature distribution obtained from equation (12) **(**Figure 4**)**. At any position of the heat source, the isotherms of various temperatures are oval shaped. Higher temperatures have smaller size ovals. The point on any isotherm that is furthest from the x-axis (or line of motion of the heat source) is at its peak temperature at that instant.

Using equation (12) and considering temperatures in terms of distance from the fusion zone boundary, it can be shown that the peak temperature for a thin plate (line source) is given

$$\frac{1}{T_p - T_0} = \frac{\sqrt{2\pi e}}{Q} \frac{\rho C_p h \mu_x Y_{HAZ}}{1} + \frac{1}{T_m - T_0} \text{ ------ (13)}$$

While that for a thick plate (point source) is

$$\frac{1}{T_p - T_0} = \frac{2\pi K \alpha e}{Q \mu_x} \{2 + (\frac{\mu_x Y_{HAZ}}{2\alpha})^2\} + \frac{1}{T_m - T_0} \text{ ------ (14)}$$

Where e = natural exponent = 2.71828, T_p is the peak or maximum temperature at a distance Y from the fusion boundary and Y is the distance from the fusion boundary at the workpiece surface.

Equations (13) and (14) are applicable to single-pass processes and have to be applied to each pass by itself. They are useful for estimating the heat-affected zone size and also for showing the effect of preheat on the HAZ size. It is evident from the equations that all parameters being constant, preheating increases the size of the HAZ. Also, the size of the HAZ is proportional to the net energy input. Thus, high-intensity processes such as laser welding generally have a smaller HAZ. A high intensity energy source results in a lower total heat input because the energy used in melting the metal is concentrated in a small region.

In general, the equation (i.e., (13) or (14)) that gives the higher computed distance from the fusion zone or higher peak temperature at a given location is the more accurate of the two.

6. Cooling Rates

The heat and the fluid flow that occur during laser processing influence the microstructures (through the grain structure and phases that are formed), residual stresses (through the thermal stresses that result from differential strains), and distortions that evolve during the process. These in turn affect the mechanical properties and thus the quality of the process, Shahram Sarkani et al. (2000).

When a material is heated to a high enough temperature, the rate at which it cools afterwards determine the grain structure and phases that are formed. These in turn affect mechanical properties such as strength and ductility. For example, high cooling rates result in a finer grain structure, which increases the strength but reduces the ductility of the material. Knowledge of cooling rate is most important for materials that are polymorphic in nature, for example, steels. This enables a variety of phases with widely different mechanical properties to be produced. It is of less interest for aluminum, for example, where the cooling rates are always high. In the general case, the cooling rate at any position at any time can be obtained by differentiating equation (12) with respect to time.

The centreline cooling rate for thick materials in three dimensional case is the cooling rate is proportional to the square of the temperature rise above the initial temperature.

$$\frac{\partial T}{\partial t} = -\frac{2\pi\alpha\mu_x}{Q}(T - T_0)^2 \text{ ------- (15)}$$

For thin plates, that is, the two-dimensional case, the centreline cooling rate is given by

$$\frac{\partial T}{\partial t} = -2\pi\alpha\rho C_p\left(\frac{\mu_x h}{Q}\right)^2 (T - T_0)^3 \text{ ------- (16)}$$

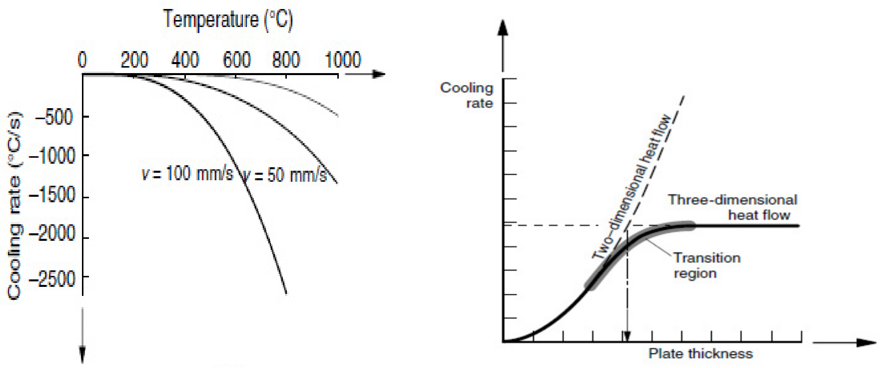

(a) (b)

Figure 5: Dependence of cooling rate on (a) traverse velocity and Representative regions for the cooling rate equations, (Elijah Kannatey-Asibu Jr, (2009))

From equations (15) and (16), the following deductions can be made,

(a) Increasing the heat input (q) reduces the cooling rate, while increasing the traverse velocity (u_x) increases the cooling rate.

(b) Increasing the initial workpiece temperature (or preheat) (T_0) reduces the cooling rate, and is more effective than increasing the heat input or reducing the traverse velocity.

(c) The cooling rate increases with an increase in plate thickness (h).

(d) A higher conductivity (k) material such as aluminum results in a higher cooling rate.

(e) The cooling rate decreases with an increasing distance (y) from the process centreline.

The last point may not be immediately obvious, unless one considers the fact that the cooling rate decreases with decreasing temperature and that from equation (12), the temperature reduces with increasing distance from the weld centreline.

Equations (15) and (16) strictly give the centreline cooling rates behind a point or line source of heat moving in a straight line at constant velocity on a flat surface and are most accurate for cooling rates at temperatures that are significantly below the melting temperature. Fortunately, the temperatures at which cooling rates are of metallurgical interest, especially for steels, are well below the melting point, and the estimates from these equations are then reasonably accurate. Furthermore, since the centreline cooling rate is only about 10% higher than in the heat-affected zone, these equations also fairly well represent cooling rates in the regions of metallurgical interest.

7. Thermal Cycles

Figure 6 shows the variation of temperature with time at three points that are located at different distances from the fusion boundary. This is referred to as the thermal cycle diagram and can be obtained by substituting the relation $\tau = \xi/u_x$ into equation (12). This will result in equations of temperature as a function of time Murugan et al. (1998). The following deductions can be made from the thermal cycle diagram:

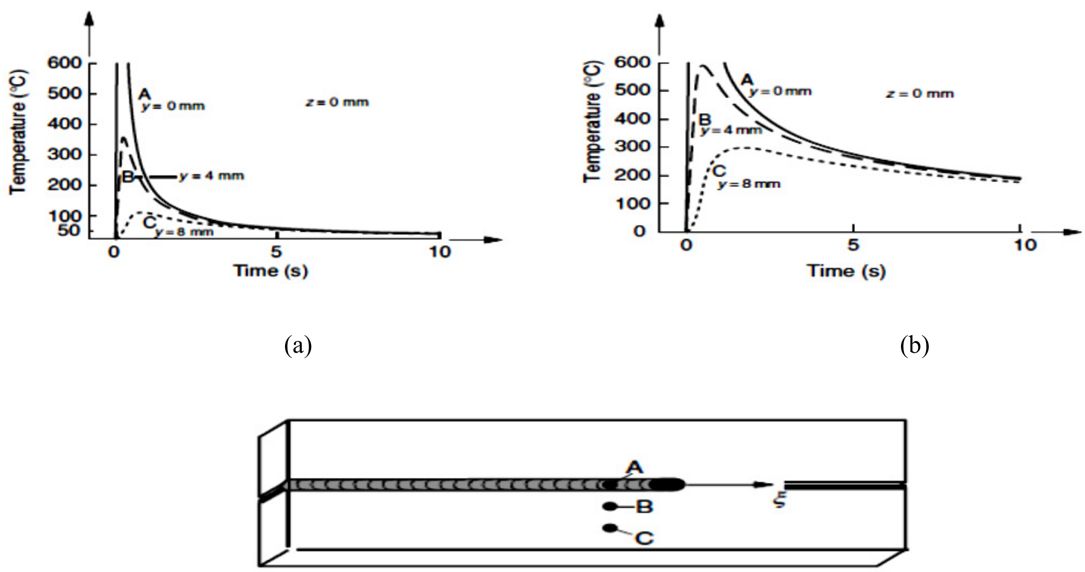

(a) (b)

(c)

Figure **6:** Thermal cycle diagrams for (a) Thin plate. (b) Thick plate. (c) Configuration showing simulation points.

1. The peak temperature decreases rapidly with increasing distance from the centreline.
2. The time required to reach the peak temperature increases with increasing distance from the centreline.
3. The rate of heating and the rate of cooling both decreases with increasing distance from the centreline.

However, the heat flow is considered only in the solid part of the workpiece, because, the predicted results are more accurate in the solid part of the workpiece.

Conclusion

The cooling rate of a material decreasing with respect to distance from the centre weld line as temperature distributed is decreasing. As the grain growth rates strongly depends on temperature distributed. An increase in temperature increases the thermal vibrational energy, which turn accelerates the net diffusion of atoms across the boundary from small to large grains or coarse grains. Subsequent, decrease in temperature slows down the boundary, but does not reverse it. Accordingly, the hardness of the weld joint is higher at the joint and starts to decrease with respect to distance from the centre weld line. Microstructure of the weld joint of a similar/dissimilar materials can be altered by particle coalescence (sometimes called as Ostwald ripening) that is directly comparable to grain growth. Since, there is very high temperature which adequate to facilitate diffusion, also, the higher temperature increases the cooling rate (the driving force) in range of super cooling, results in distribution of microstructure through an eutectic or eutectoid reaction, leads to formation of precipitation and coarse grains. The regions near the weld line undergo peak temperature and severe thermal cycle, thereby generating inhomogeneous plastic deformation and residual stress. The analytical model and the predicted results on heat flow of any solid material are directly applicable to laser welding process, but, its limited to where no melting is occurs.

References

Anawa E.M and A.G.Olabi, 2008, Review: Control of welding residual stress for dissimilar laser welded materials. Journal of material science and technology, 204, 22-33.

Andrzej Sluzalec, 2005, Theory of thermo mechanical process in welding, published by Springer, P.O. Box 17,3300 AA Dordrecht, The Netherlands.

Carslaw, H.S and Jaeger, J.C, 1959, Conduction of heat in solids, Clarendon press, Oxford.

Elijah Kannatey-Asibu Jr, 2009, principles of laser material processing, John Wiley & Sons, New Jersey.

Frewin M.R and D.A. Scott,1999, Finite element model of pulsed laser welding, Welding research supplement, 15-22.

Jaroslav Mackerle, 2004, Finite elements in the analysis of pressure vessels and piping: A bibliography (1976-1996, 1996-1998, 1999-2001, 2001-2004), International journal of pressure vessels and piping.

John Michael Dowden, 2001, The mathematics of thermal modelling: An introduction to the theory of laser material processing, Chapman and Hall/CRC, Florida.

Klaus Zimmer, 2009, Analytical solution of the laser induced temperature distribution across internal material interfaces. International journal of heat and mass transfer, 52,497-503.

Lankalapalli K.N, Jay F Tu and Mark Gartner, 1996, A model for estimating penetration depth of laser welding processes, Journal of applied Physics D: Applied Physics, 29, 1831-1841.

Mackwood, A.P and R.C. Crafer, 2005. Thermal modeling of laser welding and related process: a literature review. Optics & Laser technology, 37, 99-115.

Martinson P, S.Daneshpour, M.Kocak, S.Riekehr and P.Starson, 2009, Residual stress analysis of laser spot welding of steel sheets. Materials and Design. 30, 3351-3359.

Moraitis G.A and G.N. Labeas, 2008, Residual stress and distortion calculation of laser beam welding for aluminium lap joints. Journal of materials processing technology. 198,260-269.

Moraitis G.A and G.N.Labeas, 2009, Review: Prediction of residual stresses and distortions due to laser beam welding of butt joints in pressure vessels. International journal of pressure vessels and piping. 86,133-142.

Murugan S, P.V.Kumar, B.Raj and M.S.C.Bosc, 1998, Temperature distribution during multipass welding of plates. International Journal of Pressure Vessel and Piping, 75, 891-905.

Murugan S, P.V.Kumar, T.P.S.Gill, B.Raj and M.S.C.Bosc, 1999, Numerical modeling and experimental determination of temperature distribution during manual metal arc welding. Science and Technology of Welding and Joining. 4(6), 357-364.

Rosenthal. D, The theory of moving sources of heat and its application to metal treatments. Transactions of ASME 1946; 43(11):849–66

Shahram Sarkani, Vesselin Tritchkov and George Michaelov, 2000, An efficient approach for computing residual stresses in welded joints. Finite elements in analysis and design. 35,247-268.

Van Elsen M, M. Baelmans, P. Mercelis, J.-P. Kruth, 2007, Solutions for modelling moving heat sources in a semi-infinite medium and applications to laser material processing, International Journal of Heat and Mass Transfer, 50, 4872–4882.

Wenchun Jiang, Jianming Gong, Shandong Tu and Hu Chen,2009. Modeling of temperature field and residualstresses of vacuum brazing for stainless steel plate-fin structure. Journal of material science and technology. 209, 1105-1110.

Yilbas B. S, A.F.M.Arif,and B.J.Abdul Aleem,2010, Laser welding of low carbon steel and thermal stress analysis. Optics & Laser Technology.42, 760-768.